Title

Eyeglasses based wireless electrolyte and metabolite sensor platform

Journal

Lab on a Chip, 17(10)

ISSN

1473-0197

Authors

Sempionatto, Juliane R

Nakagawa, Tatsuo

Pavinatto, Adriana

et al.

Publication Date

2017-05-16

DOI

10.1039/c7lc00192d

Peer reviewed

HHS Public Access

Author manuscript

Lab Chip. Author manuscript; available in PMC 2018 May 16.

Published in final edited form as:

Lab Chip. 2017 May 16; 17(10): 1834–1842. doi:10.1039/c7lc00192d.

Eyeglasses based Wireless Electrolyte and Metabolite Sensor Platform

Juliane R. Sempionatto[a], **Tatsuo Nakagawa**[a], **Adriana Pavinatto**[a], **Samantha T. Mensah**[a], **Somayeh Imani**[a], **Patrick Mercier**[a], and **Joseph Wang**[a,*]

[a]School of Engineering, University of California, San Diego La Jolla, CA 92093, USA

Abstract

The demand for wearable sensors has grown rapidly in recent years, with increasing attention being given to epidermal chemical sensing. Here, we present the first example of a fully-integrated eyeglasses wireless multiplexed chemical sensing platform capable of real-time monitoring of sweat electrolytes and metabolites. The new concept has been realized by integrating an amperometric lactate biosensor and a potentiometric potassium ion-selective electrode on the two nose bridge pads of the glasses and interfacing them to a wireless electronic backbone placed on the glasses arms. Simultaneous real-time monitoring of sweat lactate and potassium levels with no apparent cross-talk is demonstrated along with wireless signal transduction. The electrochemical sensors were screen printed on a polyethylene terephthalate (PET) stickers and placed on each side of the glasses nose pads in order to monitor sweat metabolites and electrolytes. The electronic backbone on the arms of the glasses frame offers control of the amperometric and potentiometric transducers and enables Bluetooth wireless data transmission to the host device. The new glasses system offers an interchangeable-sensor feature in connection to variety of different nose-bridge amperometric and potentiometric sensor stickers. For example, the lactate bridge-pad sensor was replaced with a glucose one to offer convenient monitoring of sweat glucose. Such fully-integrated wireless "Lab-on-a-Glass" multiplexed biosensor platform can be readily expanded for the simultaneous monitoring of additional sweat electrolytes and metabolites.

Graphical abstract

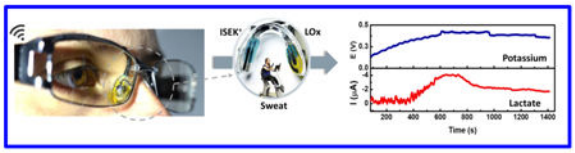

Introduction

The demand for wearable sensors has grown rapidly in recent years.[1–3] Physical sensors used to monitor heart rate,[4,5] blood pressure,[6–8] body temperature,[9] body movements,[10] are already commercially available and are now commonly used in daily life. However, new

* josephwang@ucsd.edu; Fax: +1 (858) 534 9553; Tel: +1 (858) 246 0128.

†Electronic Supplementary Information (ESI) available: See DOI: 10.1039/x0xx00000x

non-invasive chemical sensors are critically desired to expand the scope of wearable sensor technology beyond vital signs and hence to obtain a more comprehensive information about a wearer's health and performance status.[1,3,11] Several research groups have recently addressed this gap by introducing wearable chemical sensors for monitoring of metabolites, such as a lactate[12–14], glucose,[15,16] or uric acid,[17,18] and electrolytes, such as sodium,[19,20] potassium[14,20] or pH[21]. Widespread acceptance of wearable sensor technology requires the creation of products that can be easily integrated into an individual's lifestyle Most wearable chemical sensors have relied on sweat analysis in connection to flexible and temporary tattoo-like devices,[3,22,23] head bands,[24] or wrist bands.[14] Other platforms and accessories explored recently for on-body chemical sensing applications include mouthguards for saliva monitoring,[13,25] contact lenses for tear assays[26,27] or smart bandages for wound healing.[18,28] As the wearable sensor technology advances, there are urgent needs for addressing the challenges of merging the strengths of the fashion and wearable fields to create wearable fashion accessories that will lead to a widespread acceptance of wearable sensor technology.

Most existing wearable chemical sensors lack a multi-analyte detection and integration capabilities.[14,5] Gao et al. recently described a multi-sensor wristband platform to measure glucose, lactate, potassium, and sodium in sweat.[14] Lee et al. developed an integrated graphene-based patch for monitoring sweat glucose.[16] Mercier and Wang developed a hybrid Chem-Phys epidermal tattoo for simultaneous monitoring of lactate and ECG[5]. Certainly, there are urgent needs for developing new easy-to-use multi-analyte wearable chemical sensing platforms.

In this work, we demonstrate the first example of a (bio)sensor eyeglasses platform that provides an attractive platform addresses the challenge of combining a wearable chemical sensing function with eyeglass accessories through proper attention to key design and technological barriers. More specifically, we describe a fully-integrated eyeglasses wireless multiplexed chemical sensing platform for simultaneous real-time monitoring of sweat electrolytes and metabolites (Fig. 1B). Eyeglasses represent an attractive wearable platform. Since Google launched its Google Glass project, developers from around the globe have focused on introducing smart glasses as wearable computers and display devices.[29–31] However, despite of being an attractive wearable alternative to recently developed sweat sensors. The new platform, there are no reports on eyeglasses based non-invasive chemical sensors. Eyeglasses are stylish fashion accessories, and are widely worn daily by millions, compared to other accessories, e.g., wrist bands, head bands and tattoos, commonly used for wearable sensor systems. In addition, eyeglasses are common with the majority of the elderly population that requires a more frequent monitoring. The eyeglasses based sensing platform offers comfort and ease of use to the wearer. The inherent shape and weight of glasses conform well to the user face and the pressure in the nose bridge pads promotes good sensor-skin contact. In the present work we developed a new, personalized integrated eyeglasses platform for metabolites and electrolytes sensors, based on two major classes of electrochemical sensors, amperometric and potentiometric, respectively.[32] These two classes of electrochemical sensors can cover the majority of target analytes for the healthcare and fitness applications.[33] Hence, while the new concept of eyeglasses based chemical sensing is illustrated here in connection to sweat lactate and potassium monitoring, it can be readily

expanded to other important metabolites or electrolytes via a judicious selection of the enzyme or ionophore receptor, respectively, and using easily replaceable nose-bridge sticker pads.

The new wearable glasses chemical sensing platform has been realized by integrating potentiometric and amperometric sensors on the nose-bridge pads of the glasses and integrating them to a wireless electronic backbone located along the glasses arms (Fig. 1B). These nose-bridge electrochemical sensors were fabricated via conventional screen-printing technique utilizing custom-designed stencils. The three-electrode sensor patterns and contacts were printed on a polyethylene terephthalate (PET) substrate, used as replaceable sticker on the nose pad via a double-sided adhesive tape. These easily removable adhesive sensor stickers allow the user to select the target metabolite and electrolyte he/she wishes to monitor. All connections were fixed within the nose bridge pad and the glasses. Therefore, the “Lab-on-Glass” platform can thus be adjusted to meet the specific wearer's needs.

The performance of our new integrated eyeglasses wearable sensor system was demonstrated towards a continuous monitoring of the biologically important lactate and potassium. Lactate was measured amperometrically while potassium was monitored potentiometrically. Lactate is one of the most important biomarkers for assessing physical performance and well-being during physical activities. Changes in lactate sweat levels reflect the fitness level and correspond to the exercise intensity.[34,35] Sweat lactate can also be used as a marker of tissue viability and may provide warning for pressure ischemia, reflecting the insufficient oxidative metabolism and a compromised tissue viability.[36]

Monitoring the sweat electrolyte composition during exercise activity is also important. Considerable loss of electrolytes can occurs during intense exercise.[37–39] Along with chloride and sodium, potassium is one of the body's most important electrolytes. Low potassium sweat levels can indicate dehydration, that can impair the electrical impulse communication between cells, besides inducing muscle cramps.[40] Low potassium concentrations may also result in hypokalemia, the most common electrolyte abnormality, that can be life threatening in patients with cardiovascular disease.[41] Abnormal potassium concentrations and electrolyte imbalance contribute also to the risk of accidental falls in the elderly population. The monitoring of sweat potassium can thus provide prediction and alert for such abnormalities and risks.

Considering the importance of these two biomarkers, the Multi-Analyte Glasses (MAG) tested during physical activity of three healthy subjects. One of the most important considerations for simultaneous operation of two different sensors is potential cross-talk. While amperometric measurements of lactate require an applied potential of -0.1 V, monitoring the potassium levels relies on open circuit potential measurements. We demonstrate that the potential signal of the potassium sensor is completely independent of the applied potential of the lactate sensor and that the lactate and potassium on-body profiles are not affected by their simultaneous recordings. The sensor stickers of the new eyeglasses sensing platform can be readily replaced and the system can thus be readily extended for the monitoring of a wide variety of target analytes.

Materials and Methodology

Chemicals

Chitosan, acetic acid, bovine serum albumin (BSA), L-lactic acid, sodium phosphate monobasic (NaH_2PO_4), sodium phosphate dibasic (Na_2HPO_4), D (+) - glucose, glucose oxidase (GOx) from Aspergillus niger type X-S (EC 1.1.3.4), Polyurethane (PU) (Tecoflex SG-80A), potassium tetrakis (4-chlorophenyl) borate, potassium chloride, sodium chloride, calcium chloride, magnesium chloride, valinomycin (potassium ionophore I), polyvinyl chloride (PVC), bis (2-ethylhexyl) sebacate (DOS), and methanol (99.8% anhydrous) were obtained from Sigma-Aldrich (St. Louis, MO). Lactate oxidase (LOx) (activity 101 U / mg) was purchased from Toyobo Corp. (Osaka, Japan). Tetrahydrofuran (THF) with HPLC grade was purchased from Fisher Chemical (Fair Lawn, NJ). Polyvinyl butyral (PVB) B-98 was purchased from Quimidroga S.A. (Barcelona, Spain). Conductive carbon ink (E3449) and silver/silver chloride ink (E2414) were purchased from Ercon Inc. (Wareham, MA) while the Prussian-blue/graphite ink (C2070424P2) was obtained from Gwent Inc. (Torfaen, UK.) All reagents were used without further purification.

Screen printing process

The screen printing process was conducted using a semi-automatic MMP-SPM printer (Speedline Technologies, Franklin, MA), and custom stencils developed in AutoCAD software (Autodesk, San Rafael, CA),[12] and produced by Metal Etch Services (San Marcos, CA); stainless steel stencils with dimensions 12 in. × 12 in.). Lactate biosensors were screen-printed on flexible PET sheet substrate with two separate layers. First, an Ag/AgCl conductive ink was printed to prepare the reference electrode as well as the current collector for electrochemical measurements. Next, a Prussian-blue-graphite ink was printed for fabricating the working and counter electrodes (Fig. 1D). After every printing step, the printed layers were cured at 85 °C for 20 min. The working electrode transducer had a circle shape with a 3 mm diameter. Potassium sensors were screen-printed on a flexible PET sheet substrate with three separate layers. First, an Ag/AgCl conductive ink was printed as conductive collector. Next, the same ink was used to print the reference electrode. Finally, a conductive carbon ink was printed for working electrode (Fig. 1D). The printed layers were cured at 85 °C for 20 min after each printing step.

Electrodes Modification

Lactate sensors were modified as the following. Four μL of LOx (34 mg / mL) in BSA (10 mg / mL) were dropcasted on the working electrode surface and allowed to dry for two hours. Next, 4 μL of 0.5% chitosan solution in 0.1M acetic acid was casted and the electrode was left overnight at 4 ° C. The following procedure[20] was employed in the preparation of the recognition layer and reference electrode for the potassium sensor. For the reagent recognition layer, 2 mg of valinomycin were dissolved in 1 mL of THF along with 0.5 mg of potassium tetrakis (4-chlorophenyl) borate. After complete dissolution, 32.8 mg of PVC were added gradually until complete dissolution, followed by addition of 71.1 μL DOS; the solution was left stirring in vortex for one hour. After homogenization, 5 μL of the resulting cocktail solution were casted on the carbon electrode surface. For the reference electrode, 3 μL of a solution containing 78.1 mg of PVB and 50 mg NaCl in 1 mL of methanol was

dropcasted on the silver electrode. After drying, 1 μL of PU was casted on the surface in order to prevent leaching.

Electrochemical Assays

Most of the in-vitro testing of the new system were performed using benchtop electrochemical analyzers, CHI 1230A from CH Instruments (Austin, TX) and a μAutolab III from Metrohm (Utrecht, Holland). A three-electrode system was used for the amperometric sensors, the working and counter electrodes were printed using Prussian-blue/graphite ink; and the reference was the Ag/AgCl printed electrode (Fig. 1D). All solutions for the in-vitro amperometric measurements were prepared in 0.1 M PBS (pH 7.0) using DI water. Amperometric detection was performed using an applied potential of -0.1 V in order to obtain the calibration curves and the on-body measurements. A two-electrodes system was used for the potassium sensor; the modified printed Ag/AgCl electrode was used as reference electrode and the carbon-based electrode as the working electrode (Fig. 1D). The open circuit potential was recorded to obtain the calibration curves and on-body measurements.

On-Body Measurements

The epidermal evaluation on human subjects was conducted in strict compliance following a protocol approved by the institutional review board (IRB) at the University of California, San Diego. An informed consent was obtained from the human volunteer for the specific on-body experiment Three healthy volunteers (one female and two males) were asked to perform physical exercise on a stationary bicycle while wearing the MAG sensor. The nose area was cleaned prior to measurements with soap and water, then dried with isopropyl rubbing alcohol (50%). All on-body tests were performed with a wireless transceiver mounted on each inner arm of the MAG sensor system for real-time transmission of the lactate and potassium signals. Unless specified otherwise, on-body results described in the supporting information, were performed via non-wireless data acquisition made by connecting a CHI 1230A electrochemical analyzer to the potassium sensor and the μAutolab III electrochemical analyzer to the lactate sensor. The on-body experiments were performed in strict compliance with the guidelines of the Institutional Review Boards (IRB) and were approved by the Human Research Protections Program at University of California, San Diego (Project name: Epidermal Electrochemical Sensors and Biosensors. Project number: 130,003).

Wireless Transceivers

Two printed circuit board (PCB), placed on the different arms of the eyeglass frame were used to control the amperometric and potentiometric operations. The lactate and potassium sensors were connected to each of the PCBs with amperometric and potentiometric measurement capabilities, respectively, along with wireless data transmission. The controler used in both of the PCBs was a CC2541 from Texas Instrument (TI). This controller has an integrated Bluetooth Low Energy (BLE) function which enables wireless connection from the MAG sensor to a host device, such as smartwatch, smartphone or laptop. The digitized data from lactate and potassium sensors were transmitted as BLE packets via the controller to a host laptop and displayed using a custom-made graphic interface. The PCBs were

powered by a Li-ion rechargeable battery. The batteries output was regulated using low dropout regulator (LP2981 from TI) to obtain 3.0 V precise and stable power for every circuit components. The batteries have 100 mAh capacitance and size of 31 × 11.5 × 3.8 mm.

The size of the developed PCBs, 30 × 13.7 mm, can fit the frame of the glasses (Fig. 3A). On-body tests were performed using the wireless transceivers in the same fashion as was described earlier. The measured average current consumption of each the PCB during operation is 1.6 mA, which enables a battery life time of over a week with 100-mAh capacitance, assuming an 8 hours/day use. Details of the PCBs circuit boards are given in Fig. S6 and Fig. S7 (ESI†).

Lactate sensor - The LMP91000 analog frontend (AFE) chip was used as the interface for the lactate sensor. While the AFE applied a constant potential (-0.1V) between the reference and working electrodes by controlling the potential of counter electrode, it also measured the current from the working electrode and output it as an analog voltage value. The output was digitized by an analog-to-digital converter (ADC) integrated in the controller. The AFE chip is programmable through an I2C interface driven by the controller.

Potassium Sensor - A voltage follower circuit with an operational amplifier (AD8605 from Analog Devices Inc.) was used for measuring the potential signal between the reference and working electrodes. This amplifier has extremely low input bias current (<1pA) with rail-to-rail operation, enabling precise and wide-range measurement. The output of the voltage follower circuit was followed by RC low-pass filter and converted to digital value using the ADC.

Results

Eyeglasses represent an attractive platform for sweat sensing, as they offer spatially separated sensor locations on the nose pads which minimize potential cross-talk between the corresponding sensors. As a proof of concept, we were able to demonstrate below a sweat metabolite/electrolyte glasses sensor platform operating under physical exercise conditions with wireless signal transmission.

Characterization of the Lactate sensor

The fabrication and functionalization of the nose-bridge pad lactate biosensor are illustrated in Fig. 1D. There are several key analytical parameters that must be evaluated when developing a wearable sensor.[11] The new sensor should offer a fast response time, selective and reproducible response and a wide dynamic range. The lactate eyeglasses biosensor relies on the LOx-biocatalytic oxidation of lactate to pyruvate and hydrogen peroxide, and amperometric monitoring of the peroxide product. (Fig. 1C). Because of the large anodic overpotential of H_2O_2 at conventional printed solid electrodes, a Prussian-blue/graphite electrode transducer was used, allowing low-potential selective cathodic measurements at a very low potential of -0.1V (versus a Ag/AgCl reference).[42]

In order to evaluate the key parameters for the lactate sensor, the modified electrode was first characterized in-vitro using PBS (pH 7.0) over the 0-14 mM lactate concentration range, which corresponds to the range of lactate physiological concentrations in human sweat.[43] Fig. 2A displays chronamperograms for increasing lactate concentrations in 2 mM steps (a-g). Well-defined current signals are observed, with a fast stable response obtained within 30 seconds. As indicated from the corresponding calibration plot (shown in the inset), the current have a nearly linear fashion up to 8 mM and levels off above 10 mM lactate. A limit of detection (LOD) of 0.39 mM ($CL_{k=3}$) was calculated based on the IUPAC recommendation.[44] The lactate sensor inter-electrode reproducibility was evaluated. A deviation of 5-15% was found for high and low lactate concentrations, respectively (Table S1, (ESI†)). Such reproducibility is satisfactory considering the low cost electrode fabrication route. Since human sweat contains several potentially interfering compounds, e.g., ascorbic and uric acids,[43] the selectivity of the new biosensor was evaluated. Fig. 2B shows chronoamperometric curves for potentially interfering metabolites in their respective physiological concentration in sweat.[43] All four compounds: creatinine (a), ascorbic acid (b), glucose (c) and uric acid (d) exhibit negligible current signals. In contrast, a well-defined current response is observed for 4 mM lactate (e). Such high selectivity of the new eyeglasses biosensor reflects the judicious coupling of the LOx-enzymatic chitosan layer and the low-operating potential of the Prussian-blue/graphite transducer.

Potassium sensor Characterization

Potassium sensor analytical performance was evaluated using open-circuit potential measurements. A calibration curve was obtained by recording the electromotive force (E (V)) versus time, using KCl concentration ranging from 0 to 100 mM (Fig. 2C). The sensor responds instantaneously in a near-Nernstian fashion to varying potassium concentrations over the 0.1 to 100 mM range. This potential-time trace reveals that the signal reaches a steady-state within 20 s, indicating great promise for real-time monitoring of dynamic changes in the potassium sweat levels. The resulting calibration plot (shown in the inset) is linear (R^2=0.99), with a Nernstian slope of 58.0 ± 4.3 mV·decade^{-1}(n=15). The sensor offers a LOD of $10^{-3.9}$ M, calculated in accordance with IUPAC recommendation.[44] The slope and LOD are comparable to the values reported previously using similar ion-selective membranes.[20,45]

The results shown demonstrate that the new potassium sensor can be suitably used to detect potassium in human sweat, given that the average levels of potassium in human sweat varies from 6.7 μM to 38 mM.[43] The selectivity of the sensor was evaluated using the mixed solution method based on IUPAC recommendation[46] using a fixed interference of 10 mM for sodium, magnesium and calcium chlorides corresponding to the physiological concentration range.[43] The results, shown in Fig. S1 (ESI†), illustrate that the potassium sensor maintains Nernstian behaviour in the presence of interfering ions (with slopes of K_{Na} = 61.39, K_{Ca} = 65.65 and K_{Mg} = 59.36 in the presence of Na, Ca and Mg, respectively). The calculated selectivity coefficients for Na^+, Ca^{2+} and Mg^{2+}, are -3.2, -5.0 and -4.9, respectively, which are in close agreement with reported data.[47]

A reversible and rapid response is essential for the performance of the epidermal potassium sensor, due to the dynamic changes of sweat electrolytes concentrations.[38,48] It is thus important to test the changes on the response of the eyeglasses sensor when potassium activity fluctuates using hysteresis effects. Fig. 2D displays the results of such carry-over test from the dynamic response recorded upon alternating cycles of 0, 0.1, 10 and 100 mM KCl solutions over a 5 min period. The potentiometric sensor displays a nearly-reversible response to these rapidly varying potassium concentrations with negligible carry-over effects.

Wireless Real-time Monitoring of Electrolyte and Metabolites

In order to realize the integration of the MAG multiplex system, both potassium and lactate electrodes were connected each to a printed circuit board (PCB) located on each of the inner arm of the glasses frame (Fig. 3A). Details of both electronic boards are given in the experimental section. The PCBs were able to collect data from the individual sensors and transmit them wirelessly via Bluetooth to a laptop. The potassium board recorded the OCP while the lactate board measured the amperometric response under a potential of -0.1V. In-vitro data calibration curves using the wireless boards were obtained in accordance with the experimental setup shown in Fig. 3B. Fig. 3C displays the potential-time response of the potassium sensor to increasing KCl concentrations from 0.01 to 10 mM. Fig. 3D displays the lactate sensor response to increasing lactate concentration from 0 to 10 mM. The corresponding potassium and lactate calibration curves (shown in the insets Fig. 3C and 3D, respectively) are consistent with the calibration curves obtained using bench top instrumentation (Fig. 2A and 2C).

In addition, the sweat replacement rate was calculated using the best-case limit single-centred flow model [49], based on a mean sweat rate of ~ 3-4 mg $min^{-1}cm^{-250}$; using the nose pad dimensionssize, (0.5 cm × 0.8 cm × 30 μm) the calculated sampling interval for the MAG device is less than 30 seconds. Tthe refresh rate of sweat is thus fast enough to perform a real-time monitoring of the analytes.

Following the in-vitro characterization, the lactate and potassium sensors were evaluated by placing them on the nose pad of the glasses (Fig. 1C) and performing on-body measurements during physical (cycling) activity. Fig. 4A displays two sets of on-body lactate (a, a′) and potassium (b, b′) signals, recorded simultaneously during exercise activity for two different volunteers using the on-body configuration shown in Fig. 4B. The same glasses prototype was used for all on-body experiments; the sensor/skin contact was made by adjusting the aperture of the nose bridge to each volunteer's nose features. The glasses weight and nose bridge pressure were sufficient for ensuring a stable reproducible signal. A calibration curve was obtained for each sensor prior to the on-body tests. The sweat potassium response during on-body test (Fig. 4Aa,a′) is in agreement with previously published studies regarding of potentiometric perspiration sensors.[51-53] At the beginning of exercise, no sweat is present and, as the exercise continues more sweat is generated, leading to rising potassium signal. Within few minutes (~10 min.), the sweat generated is sufficient for establishing a stable OCP. The potential measured from this point corresponded to physiological potassium ion concentrations.[43]

The on-body sweat lactate profile (Fig. 4Ab,b′) is also in accordance with earlier studies.[12,52] At the beginning of exercise, little or no sweat is present and the amperometric sensor measures only a background current. Perspiration begins at approximately 400 sec, leading to a rapidly increasing lactate signal that reaches a maximum value around 700 sec. The lactate profile varies in accordance with the intensity of exercise; greater intensity produces a larger sweat lactate signal. In order to further evaluate the performance of the potassium and lactate sensors, bench top instrumentation was also used for the on-body test besides the wireless boards, in order to compare both results. The sweat potassium response of three different volunteers was thus individually monitored, and the results obtained (shown in Fig. S2 ESI†) were consistent with those obtained with the MAG device.

For the individual lactate sweat analysis, a control sensor with the same surface formulation (except for the absence of LOx) was employed side-by-side with the LOx-containing lactate biosensor. These LOx and control sensors were fixed on each nose pads of the glasses and the corresponding current profiles were recorded simultaneously. As expected, the lactate sensor displayed a well-defined lactate sweat current-time profile while the control side displayed only a background current (Fig. S3 ESI†). Simultaneous sweat potassium and lactate response were also evaluated using two benchtop instruments, as shown in Fig. S4 (ESI†) for three subjects (A,D,G). The two sensors were calibrated prior to the on-body deployment, as illustrated from the potassium (B,E,H) and lactate (C,F,I) calibrations plots of Fig. S4 (ESI†).

The simultaneous on-body measurements of potassium and lactate performed using the MAG device were comparable to the response of a bench-top equipment. The similar response profiles observed with both the PCB and benchtop instrumentation reflects the quality of the new electronic interface. As was discussed earlier, one of the major challenges in designing multiplex sensing system is the potential cross-talk between the individual sensors. Cross-talk is of particular concern for multiplexed sensors employing controlled-potential amperometric detection, and potentiometric detection that measures potential signal. While cross-talk can be avoided by geometric separation of the sensors,[5] As expected from the physical separation of the 2 sensors and their separate circuit boards, cross talk between the sensors is minimal. The cross-talk between the amperometric and potentiometric sensors in the wireless MAG was investigated (Fig. S5 (ESI†)). During exercise, the sweat lactate and potassium were measured simultaneously, while the lactate PCB was turned ‘on’ and ‘off’ several times and the potassium signal was recorded without interruption. No interference was found in the potassium response due to these On/Off operation of the lactate biosensor, indicating minimal cross-talk and successful integration of a wireless multiplex sensor onto a glasses. This cross-talk experiment demonstrates also the fast and stable response, with rapid return to the previously recorded signal.

The new glasses sensing platform allows convenient replacement of the bridge-pad sensor stickers in connection to variety of different amperometric and potentiometric sensor stickers. For example, replacing the lactate bridge-pad sensor with a glucose one, offered convenient monitoring of sweat glucose. Few recent studies indicated the relevance of sweat glucose for blood glucose management.[14,16] Two healthy volunteer were randomly selected to perform this glucose test. Before exercising, the subjects were asked to consume a soft

drink with high sugar content (39 g). After waiting for 10 min, the subjects started the stationary cycling activity while monitoring the sweat glucose levels continuously for 30 minutes using the eyeglasses based biosensor. Fig. 4Ca, a′ displays the current-time profile from the sweat glucose on-body experiment. A clear increase in the glucose signal is observed following ~10 min cycling (start of sweating). The current increases rapidly to reach its maximum value at ~750 sec, and starts to decrease thereafter, within ~1000 sec. A control sensor (without GOx), shown in Fig. 4Db,b′, displays only the background current. For one of the subjects, before the on-body test, the blood glucose level was measured with a commercial glucose meter (126 mg/dl) and a calibration curve for the glucose sensor was obtained (Fig. 3E). The sweat glucose level was thus estimated to be ~0.2 mM (Fig. 4Ca); this value is in agreement with the expected blood-sweat glucose correlations.[54] Both amperometric and potentiometric sensors maintained good performance during prolonged operations of few hours, as illustrated in Fig. S4 (ESI†). Considering their low fabrication costs, good reproducibility and convenient replacement, new sensors can be readily used for new on-body measurement cycles.

Conclusions

We have demonstrated for the first time a fully-integrated wireless eyeglasses-based multiplexed biosensor platform for simultaneous real-time monitoring of sweat electrolytes and metabolites. Eyeglasses have been shown extremely attractive wearable platform for performing on-body chemical sensing. Such wearable sensing device has been realized by incorporating amperometric and potentiometric sensors on each of the nose bridge pads of the glasses and integrating them to a wireless electronic backbone located along the arms of the glasses frame. The eyeglasses based chemical sensing platform ntegrates all the required functionalities in a practical form-factor and offers comfort and ease of use to the wearer while ensuring good sensor-skin contact. Sweat lactate and potassium were measured simultaneously on-body in real time during exercise activity using the wireless MAG device with good agreement to data recorded with a bench-top instrumentation. The new eyeglasses sensing platform offers convenient replacement of the adhesive sensor stickers towards amperometric and potentiometric monitoring of a wide variety of metabolites and electrolytes. Further improvements could be achieved by integrating temperature and pH microsensors onto the MAG system (for compensating skin temperature or pH effects), as well using fluidics to control the sweat flow. The new non-invasive chemical sensing platform provides an attractive alternative to recently developed sweat sensing devices, and hence fills current gaps in wearable chemical sensor technology, as desired for mobile health monitoring and remote diagnostics. Such tech/fashion integration is expected to lead to a widespread acceptance of wearable sensor technology by the general public.

Supplementary Material

Refer to Web version on PubMed Central for supplementary material.

Acknowledgments

This work was supported by the Defense Threat Reduction Agency Joint Science and Technology Office for Chemical and Biological Defense (HDTRA 1-16-1-0013) and the National Institute of Biomedical Imaging and

Bioengineering of NIH (R21EB019698). J.R.S. acknowledges fellowships from CNPq (number- 216981/2014-0) and A.P. acknowledges FAPESP-BEPE (2015/08033-0).

References

1. Bandodkar AJ, Wang J. Trends Biotechnol. 2014; 32:363–371. [PubMed: 24853270]
2. Mukhopadhyay SC. IEEE Sens J. 2015; 15:1321–1330.
3. Bandodkar AJ, Jia W, Wang J. Electroanalysis. 2015; 27:1–12.
4. Takamatsu S, Lonjaret T, Crisp D, Badier JM, Malliaras GG, Ismailova E. Sci Rep. 2015; 5:15003. [PubMed: 26446346]
5. Imani S, Bandodkar AJ, Mohan AMV, Kumar R, Yu S, Wang J, Mercier PP. Nat Commun. 2016; 7:11650. [PubMed: 27212140]
6. Choong CL, Shim MB, Lee BS, Jeon S, Ko DS, Kang TH, Bae J, Lee SH, Byun KE, Im J, Jeong YJ, Park CE, Park JJ, Chung UI. Adv Mater. 2014; 26:3451–3458. [PubMed: 24536023]
7. Wang X, Gu Y, Xiong Z, Cui Z, Zhang T. Adv Mater. 2014; 26:1336–1342. [PubMed: 24347340]
8. Park J, Kim JK, Patil S, Park JK, Park S, Lee DW. Sensors. 2016; 16:809.
9. Trung TQ, Ramasundaram S, Hwang BU, Lee NE. Adv Mater. 2016; 28:502–509. [PubMed: 26607674]
10. Son D, Lee J, Qiao S, Ghaffari R, Kim J, Lee JE, Song C, Kim SJ, Lee DJ, Jun SW, Yang S, Park M, Shin J, Do K, Lee M, Kang K, Hwang CS, Lu N, Hyeon T, Kim DH. Nat Nanotechnol. 2014; 9:397–404. [PubMed: 24681776]
11. Bandodkar AJ, Jeerapan I, Wang J. ACS Sensors. 2016; 1:464–482.
12. Jia W, Bandodkar AJ, Valdés-Ramírez G, Windmiller JR, Yang Z, Ramírez J, Chan G, Wang J. Anal Chem. 2013; 85:6553–6560. [PubMed: 23815621]
13. Kim J, Valdés-Ramírez G, Bandodkar AJ, Jia W, Martinez AG, Ramírez J, Mercier P, Wang J. Analyst. 2014; 139:1632–6. [PubMed: 24496180]
14. Gao W, Emaminejad S, Nyein HYY, Challa S, Chen K, Peck A, Fahad HM, Ota H, Shiraki H, Kiriya D, Lien DH, Brooks GA, Davis RW, Javey A. Nature. 2016; 529:509–514. [PubMed: 26819044]
15. Bandodkar AJ, Jia W, Yard C, Wang X, Ramirez J, Wang J, Yardımcı C, Wang X, Ramirez J, Wang J. Anal Chem. 2015; 87:394–8. [PubMed: 25496376]
16. Lee H, Choi TK, Lee YB, Cho HR, Ghaffari R, Wang L, Choi HJ, Chung TD, Lu N, Hyeon T, Choi SH, Kim DH. Nat Nanotechnol. 2016; 11:566–572. [PubMed: 26999482]
17. Kim J, Imani S, de Araujo WR, Warchall J, Valdés-Ramírez G, Paixão TRLC, Mercier PP, Wang J. Biosens Bioelectron. 2015; 74:1061–1068. [PubMed: 26276541]
18. Kassal P, Kim J, Kumar R, De Araujo WR, Steinberg IM, Steinberg MD, Wang J. Electrochem commun. 2015; 56:6–10.
19. Bandodkar AJ, Molinnus D, Mirza O, Guinovart T, Windmiller JR, Valdés-Ramírez G, Andrade FJ, Schöning MJ, Wang J. Biosens Bioelectron. 2014; 54:603–609. [PubMed: 24333582]
20. Parrilla M, Cánovas R, Jeerapan I, Andrade FJ, Wang J. Adv Healthc Mater. 2016; 5:996–1001. [PubMed: 26959998]
21. Bandodkar AJ, Hung VWS, Jia W, Valdés-Ramírez G, Windmiller JR, Martinez AG, Ramírez J, Chan G, Kerman K, Wang J. Analyst. 2013; 138:123–8. [PubMed: 23113321]
22. Kim J, Jeerapan I, Imani S, Cho TN, Bandodkar A, Cinti S, Mercier PP, Wang J. ACS Sensors. 2016; 1:1011–1019.
23. Koh A, Kang D, Xue Y, Lee S, Pielak RM, Kim J, Hwang T, Min S, Banks A, Bastien P, Manco MC, Wang L, Ammann KR, Jang KI, Won P, Han S, Ghaffari R, Paik U, Slepian MJ, Balooch G, Huang Y, Rogers JA. Sci Transl Med. 2016; 8:366ra165–366ra165.
24. Jia W, Wang X, Imani S, Bandodkar AJ, Ramírez J, Mercier PP, Wang J. J Mater Chem A. 2014; 2:18184–18189.
25. Kim J, Imani S, De Araujo WR, Warchall J, Valdés-Ramírez G, Paixão TRLC, Mercier PP, Wang J. Biosens Bioelectron. 2015; 74:1061–1068. [PubMed: 26276541]
26. Mitsubayashi K, Arakawa T. Electroanalysis. 2016; 28:1170–1187.

27. Pankratov D, González-Arribas E, Blum Z, Shleev S. Electroanalysis. 2016; 28:1250–1266.
28. Guinovart T, Valdés-Ramírez G, Windmiller JR, Andrade FJ, Wang J. Electroanalysis. 2014; 26:1345–1353.
29. Glauser W. Can Med Assoc J. 2013; 185:1385–1385. [PubMed: 24082019]
30. Muensterer OJ, Lacher M, Zoeller C, Bronstein M, Kübler J. Int J Surg. 2014; 12:281–289. [PubMed: 24534776]
31. Zhang YS, Busignani F, Ribas J, Aleman J, Rodrigues TN, Shaegh SAM, Massa S, Rossi CB, Taurino I, Shin SR, Calzone G, Amaratunga GM, Chambers DL, Jabari S, Niu Y, Manoharan V, Dokmeci MR, Carrara S, Demarchi D, Khademhosseini A. Sci Rep. 2016; 6:22237. [PubMed: 26928456]
32. Wang, J. Analytical Electrochemistry. John Wiley & Sons, Inc; Hoboken, NJ, USA: 2006.
33. Singh P, Pandey SK, Singh J, Srivastava S, Sachan S, Singh SK. Nano-Micro Lett. 2016; 8:193–203.
34. Pilardeau P, Vaysse J, Garnier M, Joublin M, Valeri L. Br J Sports Med. 1979; 13:118–21. [PubMed: 486883]
35. Pilardeau PA, Lavie F, Vaysse J, Garnier M, Harichaux P, Margo JN, Chalumeau MT. J Sports Med Phys Fitness. 1988; 28:247–52. [PubMed: 3230906]
36. Polliack A, Taylor R, Bader D. J Rehabil Res Dev. 1997; 34:303–8. [PubMed: 9239623]
37. Mao IF, Chen ML, Ko YC. Arch Environ Health. 2010; 56:271–277.
38. Maughan RJ, Shirreffs SM. J Sports Sci. 1997; 15:297–303. [PubMed: 9232555]
39. Maughan RJ, Leiper JB, Shirreffs SM. BrJ Spors Med. 1997; 31:175–182.
40. Maughan RJ. J Sport Sci. 1991; 9:117–142.
41. Gennari FJ. N Engl J Med. 1998; 339:451–458. [PubMed: 9700180]
42. Ricci F, Palleschi G. Biosens Bioelectron. 2005; 21:389–407. [PubMed: 16076428]
43. Harvey CJ, LeBouf RF, Stefaniak AB. Toxicol Vitr. 2010; 24:1790–1796.
44. Long GL, Winefordner JD. Anal Chem. 1983; 55:712–724.
45. Guinovart T, Parrilla M, Crespo GA, Rius FX, Andrade FJ. Analyst. 2013; 138:5208. [PubMed: 23775189]
46. Umezawa Y, Bühlmann P, Umezawa K, Tohda K, Amemiya S. Pure Appl Chem. 2000; 72:1851–2082.
47. Bakker E. J Electrochem Soc. 1996; 143:L83.
48. Buono MJ, Ball KD, Kolkhorst FW. J Appl Physiol. 2007; 103:990–4. [PubMed: 17600161]
49. Sonner Z, Wilder E, Heikenfeld J, Kasting G, Beyette F, Swaile D, Sherman F, Joyce J, Hagen J, Kelley-Loughnane N, Naik R. Biomicrofluidics. 2015; 9
50. Vimieiro-Gomes AC, Magalhães FC, Amorim FT, Machado-Moreira CA, Rosa MS, Lima NRV, Rodrigues LOC. Brazilian J Med Biol. 2005; 38:1133–9.
51. Parrilla M, Ferré J, Guinovart T, Andrade FJ. Electroanalysis. 2016; 28:1267–1275.
52. Gao W, Emaminejad S, Nyein HYY, Challa S, Chen K, Peck A, Fahad HM, Ota H, Shiraki H, Kiriya D, Lien DH, Brooks GA, Davis RW, Javey A. Nature. 2016; 529:509–514. [PubMed: 26819044]
53. Bandodkar AJ, Molinnus D, Mirza O, Guinovart T, Windmiller JR, Valdés-Ramírez G, Andrade FJ, Schöning MJ, Wang J. Biosens Bioelectron. 2014; 54:603–609. [PubMed: 24333582]
54. Moyer J, Wilson D, Finkelshtein I, Wong B, Potts R. Diabetes Technol Ther. 2012; 14:398–402. [PubMed: 22376082]

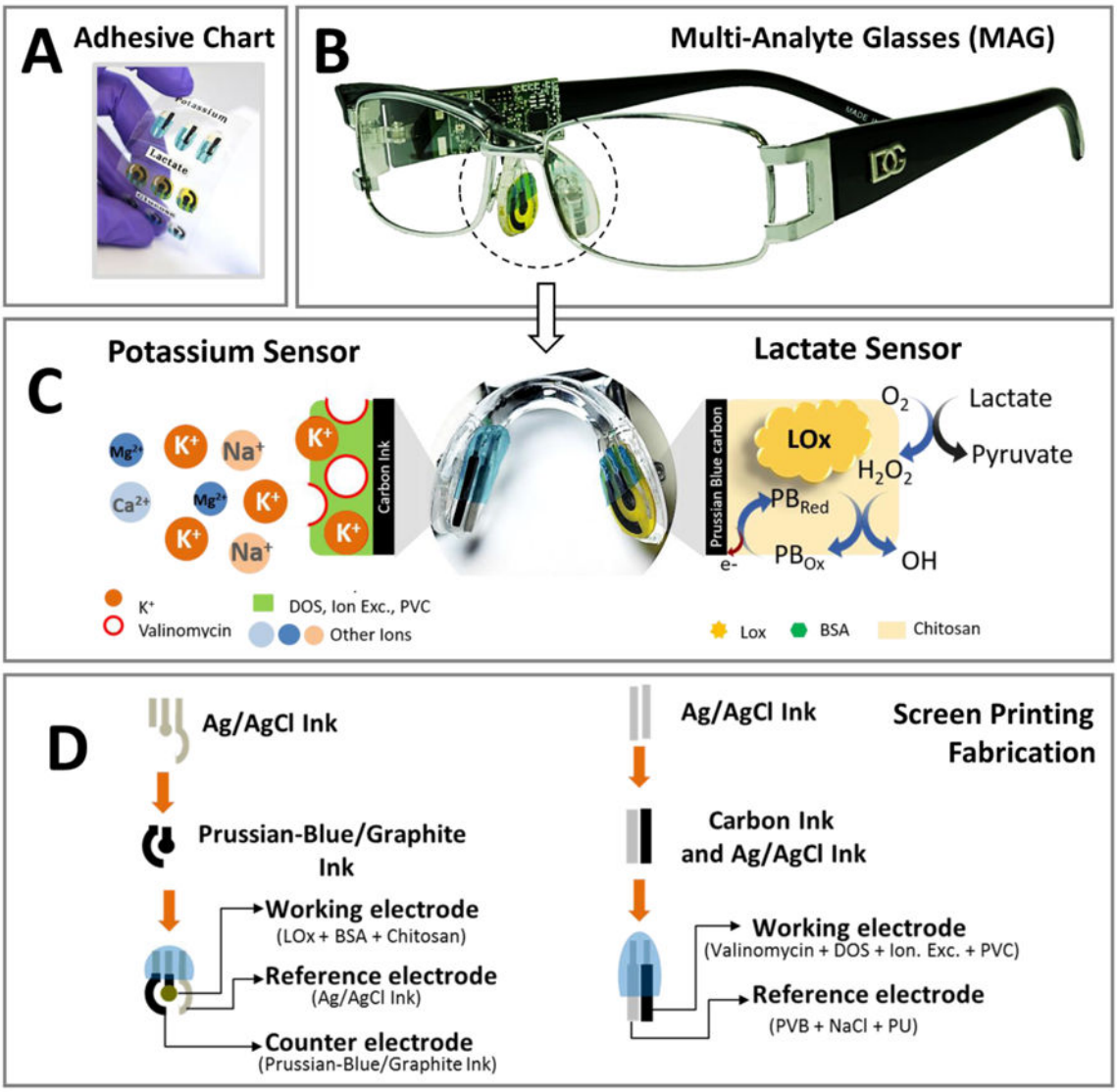

Fig. 1.

A) Photograph of interchangeable sticker printed sensors. B) Photograph of the eyeglasses biosensor system integrated with wireless circuit board along the arms. C) Nose pad electrochemical sensors with schematic of potassium sensor (left) and lactate sensor (right), along with the corresponding recognition and transduction events. D) Schematic of screen printing process steps and electrode modification for the lactate sensor (left) and potassium sensor (right).

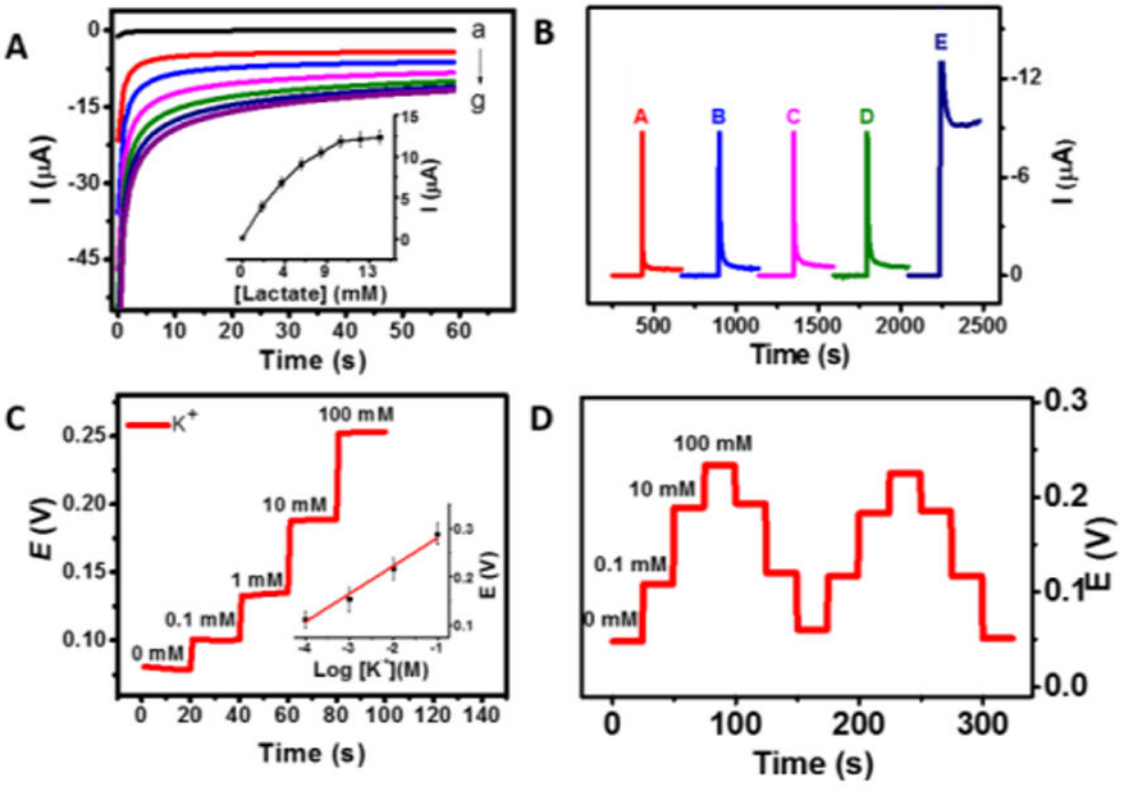

Fig. 2.

A) Chronoamperometric response for 0, 2, 4, 6, 8, 10, 12 and 14 mM lactate along with the corresponding calibration plot. Standard deviation n=3. B) Selectivity study: Response to (a) 84 μM creatinine, (b) 10 μM ascorbic acid, (c) 0.17 mM glucose, (d) 59 μM uric acid, and (e) 4 mM lactate. C) Response of the potassium sensor using 0.1, 1, 10 and 100 mM KCl, along with the corresponding calibration plot. D) Hysteresis curve (carry-over study) for the potentiometric sensor using varying potassium concentrations.

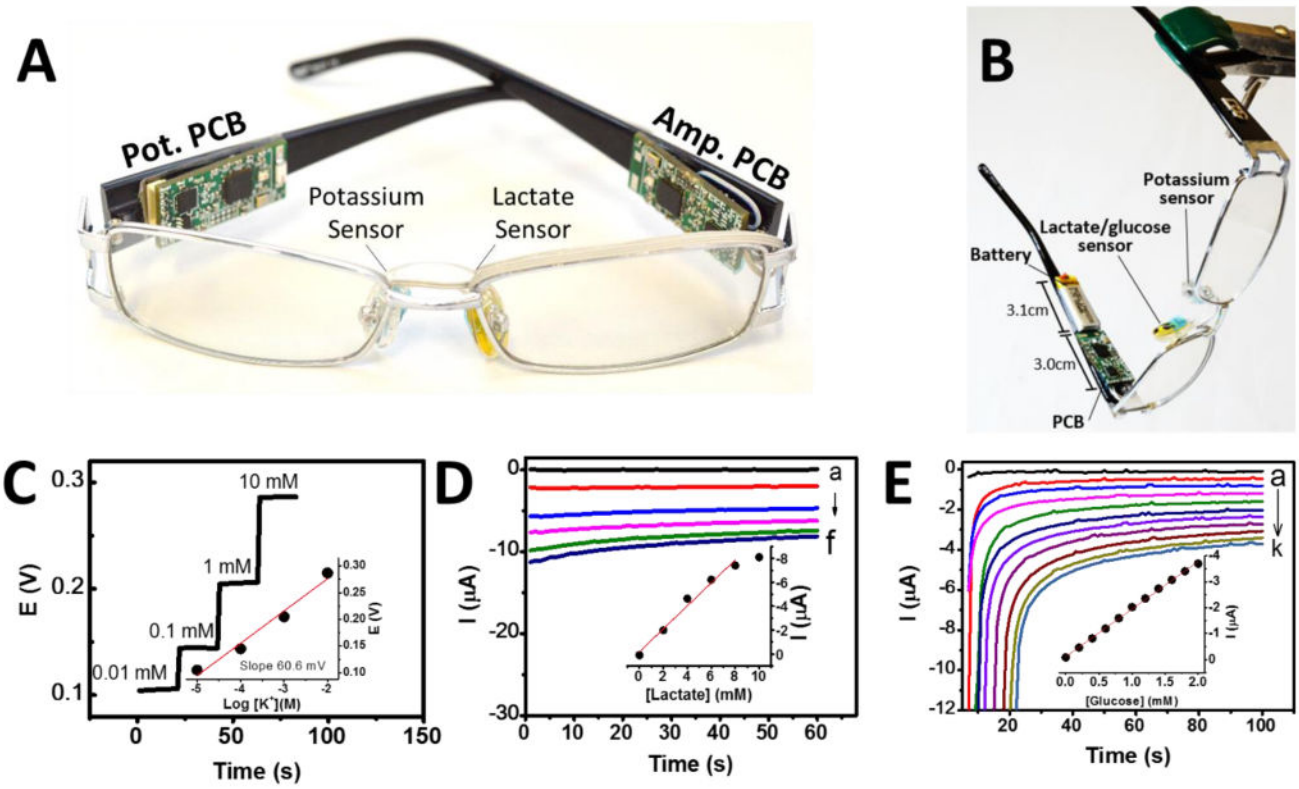

Fig. 3.

A) MAG biosensor device with both potentiometric (Pot.) and amperometric (Amp.) PCBs boards. B) Setup for in-vitro measurements using the wearable MAG biosensor device. C) Response of the potassium sensor to 0.01, 0.1, 1 and 10 mM KCl in DI water. D) Response of the lactate biosensor to increasing lactate concentration from 0 to 10 mM, with 2 mM increments in PBS (pH 7). E) Response of the glucose sensor to increasing glucose concentration from 0 to 2 mM with 0.2 mM steps in PBS (pH 7). Insets C, D and E: corresponding calibration plots for potassium, lactate and glucose sensors, respectively.

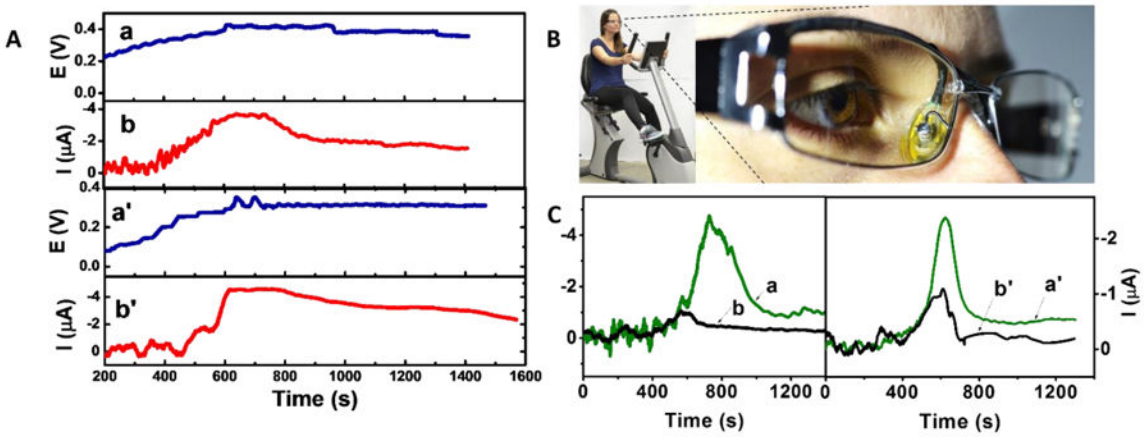

Fig. 4.

Wireless measurements using the PCBs boards. A) Simultaneous sweat potassium (a,a′) and lactate (b,b′) signals recorded during cycling exercise of two different volunteers via wireless using the MAG device.. B) Female volunteer cycling a stationary bike using the wireless MAG device C) Simultaneous measurements of sweat glucose response for glucose sensor (a,a′) and control (no-enzyme) sensor (b, b′), obtained with two different volunteers, during exercise using the MAG device.